Highly Sensitive and Stable SERS Substrate Fabricated by Co-sputtering and Atomic Layer Deposition

Guilin Yin[1,2†], Shiheng Bai[1,2†], Xinglong Tu[1], Zheng Li[1,2], Yanpeng Zhang[1,2], Weiming Wang[3], Jing Lu[2*] and Dannong He[1,2]

Abstract

In this study, we develop a facile method to fabricate highly sensitive and stable surface-enhanced Raman scattering (SERS) substrate, which is realized by combining co-sputtering with atomic layer deposition technology. To accomplish the SERS substrate preparation, we firstly utilized co-sputtering silver and aluminum on glass slides to form uniform discontinuous Ag film by removing Al later, which acted as SERS active moiety and presented high sensitivity in glycerin detection. After coating an ultrathin TiO_2 layer via atomic layer deposition (ALD), the samples could further enhance the Raman signal due to the chemical effect as well as the long-range effect of the enhanced electromagnetic field generated by the encapsulated Ag nanoparticles (NPs). Besides, the coated sample could maintain the significant enhancement in air condition for more than 30 days. The high stability is induced by TiO_2 layer, which efficiently prevents Ag NPs from surface oxidation. This highly sensitive and stable SERS substrate might highlight the application of interface state investigation for exploring novel liquid lubricating materials.

Keywords: Ag nanoparticles, SERS, TiO_2, Co-sputtering, ALD

Introduction

Since surface-enhanced Raman scattering (SERS) was firstly reported [1], it has attracted lots of interests in detecting various analytes at extremely low concentrations due to some excellent characters such as high sensitivity, quick response, noninvasive analysis, and fingerprint recognition [2–5]. Typically, SERS contributed more and more in surface state analysis with tremendous development of in situ and real-time detection in recent years, which might open a new window for surface research [6, 7]. As a result, different materials have been explored as active SERS species, including Au, Ag, Cu, Pt, and so on [8–11]. Compared with other materials, Ag nanostructures could lead to a superior enhancement factor resulting from their unique plasmonic properties [12–14].

According to previous reports, researchers have made great efforts to enhance the SERS effect in Ag nanostructures by controlling their shapes, sizes, quantities, and arrangement on solid slides [15]. Many novel Ag nanostructures such as spheres, cubes, octahedrons, and wires have been developed to maximize their SERS capabilities and uniformities [16–19]. Furthermore, different methods have been tried to fabricate these Ag nanostructures on glass or silicon substrates, such as electron-beam lithography, reactive ion etching, immersion plating, and chemical reduction [20–22]. However, there are few reports about Ag nanostructure-based SERS substrate for interface research applied in super lubricating liquids, for challenges such as complex and costly fabrication process, easy aggregation, and rapid surface oxidation when exposed to ambient conditions. These would result in SERS activity loss of the substrate in a short time [23]. Moreover, the humidity rate of liquid super lubricate will quickly decay of the Raman signal enhancement, influencing the interface state analysis during the friction process [24, 25].

* Correspondence: jinglu2004@163.com
†Guilin Yin and Shiheng Bai contributed equally to this work.
²National Engineering Research Center for Nanotechnology, No. 28 East Jiangchuan Road, Shanghai 200241, People's Republic of China
Full list of author information is available at the end of the article

Herein, a facile method is developed to fabricate highly sensitive and stable SERS substrate based on Ag nanoparticles (NPs) by combining co-sputtering with atomic layer deposition technology for glycerin detection, which played an important role in the liquid super lubricating system [24, 25]. To obtain uniform Ag NPs on a glass slide as SERS active moiety, different content of aluminum was co-sputtered with silver firstly and was removed from glass slides by phosphate later. Noticeably, high SERS performance is realized for glycerin detection by modulating deposition power rate of silver and aluminum targets due to their significant influence on the size and distribution of Ag NPs [26, 27]. We also evaluated the stability of SERS performance by comparing the spectrum collected in different duration. In particular, after coating the active moiety Ag NPs a protectiveTiO$_2$ layer via atomic layer deposition (ALD), the sample can maintain an excellent SERS performance in air condition for more than 30 days due to impeding surface oxidation and prohibit aggregation of Ag NPs. Moreover, this further enhancement effect is closely related with the TiO$_2$ layer. We ascribe this to the exponential attenuation of strong electromagnetic field with the increasing thickness of the "spacer" film. The results might present a new perspective in the field of interface analysis through employing the SERS detection.

Methods
Fabrication of Ag NPs on Glass by Co-sputtering
Conventional glass slides (15 × 15 mm, Sail Brand) were ultrasonically cleaned orderly in acetone, ethanol, and deionized water, each for 15 min to remove the surface contaminants prior to use. The Ag NPs were deposited on pre-cleaned glass substrates at room temperature by co-sputtering silver and aluminum firstly (LLJGP-450 Magnetron Sputtering System, SKY Technology Development Co., Ltd., China). Both silver and aluminum targets are of high purity (> 99.99%) with a diameter of 60 mm (purchased from SKY Technology Development Co., Ltd., China). The base pressure of the vacuum system prior to deposition was better than 4.0×10^{-4} Pa, and the working argon pressure of 0.8 Pa was maintained during deposition. Noticeably, during the co-sputtering process, the power ratio was modulated by the DC magnetron sputtering power of aluminum target when the radio frequency power of the silver target was maintained at 30 W. The Al NPs were removed by immersing the glass slides in diluted phosphate acid solution (0.5 M) for 4 h. After this, the glass slides with Ag NPs were rinsed with deionized water for five times to remove absorbed phosphate or aluminum components. After drying the glass slides with nitrogen, uniform Ag NPs have been left as SERS active moiety before coating a thin protective layer. All chemicals were analytical reagents and used as received without further purification (purchased from Sinopharm Chemical

Reagent Co., Ltd., China). Deionized water was obtained from the water purification system in our laboratory.

Preparation of Protective TiO$_2$ Layer via Atomic Layer Deposition
An ultrathin TiO$_2$ layer was grown on the as-prepared SERS active moiety via ALD using a commercial flow-type ALD reactor (Picson-100). High-purity chemical precursors, TiCl$_4$ (Alfa Aesar 99.99%), and high-purity water were employed as Ti and O sources, which were alternately pumped to the reaction chamber using ultrapure N$_2$ (99.999%) as process, and carrier gas during deposition process after the chamber was maintained at a pressure of 10 hPa and 300 °C. The pulse and purge times of TiCl$_4$ were 400 ms and 5 s, whereas the pulse and purge times of H$_2$O were 200 ms and 8 s. The pressure in the reactor varied between 1.5 and 3 hPa during the pulsing of TiCl$_4$ and H$_2$O, respectively. The thickness of the TiO$_2$ coating layer was controlled by deposition cycles with a growth rate of 0.04 nm per cycle.
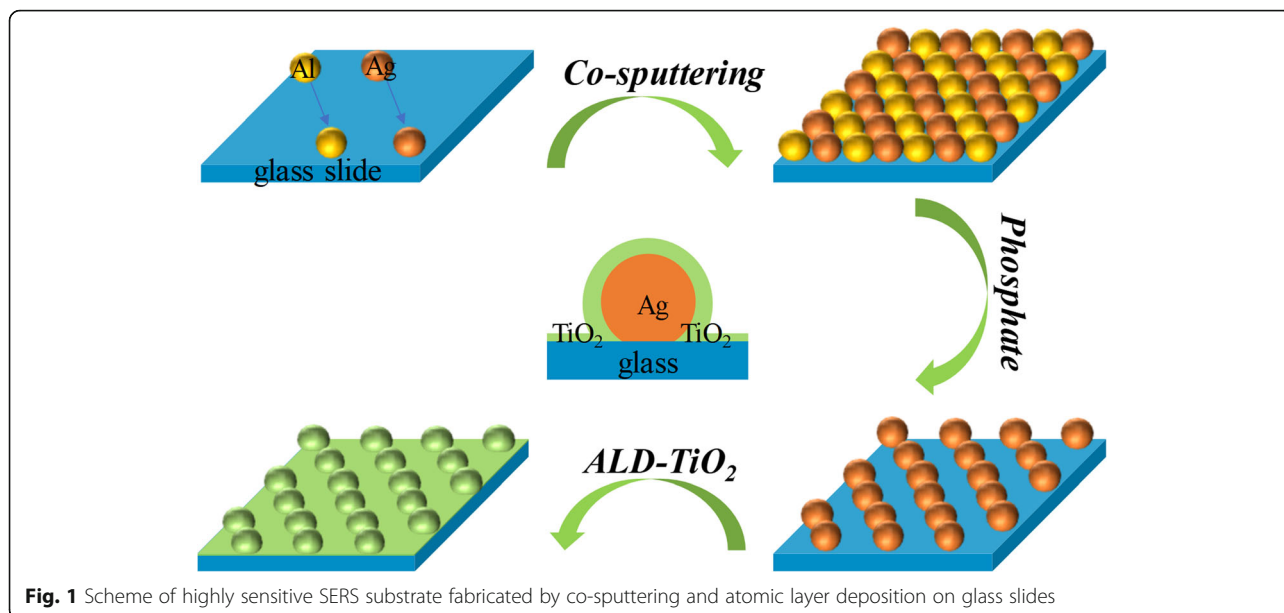
Characterization of Substrates and SERS Measurements
Field emission scanning electron microscope (FE-SEM, S-4800, Hitachi, Japan) was used to observe the surface morphology and structure of prepared SERS substrates. The atom information of substrates was determined by an energy dispersive spectroscopy (EDS, ORAN System SIX). UV-visible absorption spectra (Perkin Elmer: Lambda2) was performed to investigate the absorbance of the prepared Ag NPs. The SERS performance was tested on a confocal microscope Raman system (Renishaw: Invia-reflex) with a 532-nm diode laser and 1800 lines/mm grating observed through a × 50 LWD objective. Glycerol solution was used as a probing molecule during all SERS performance evaluation.
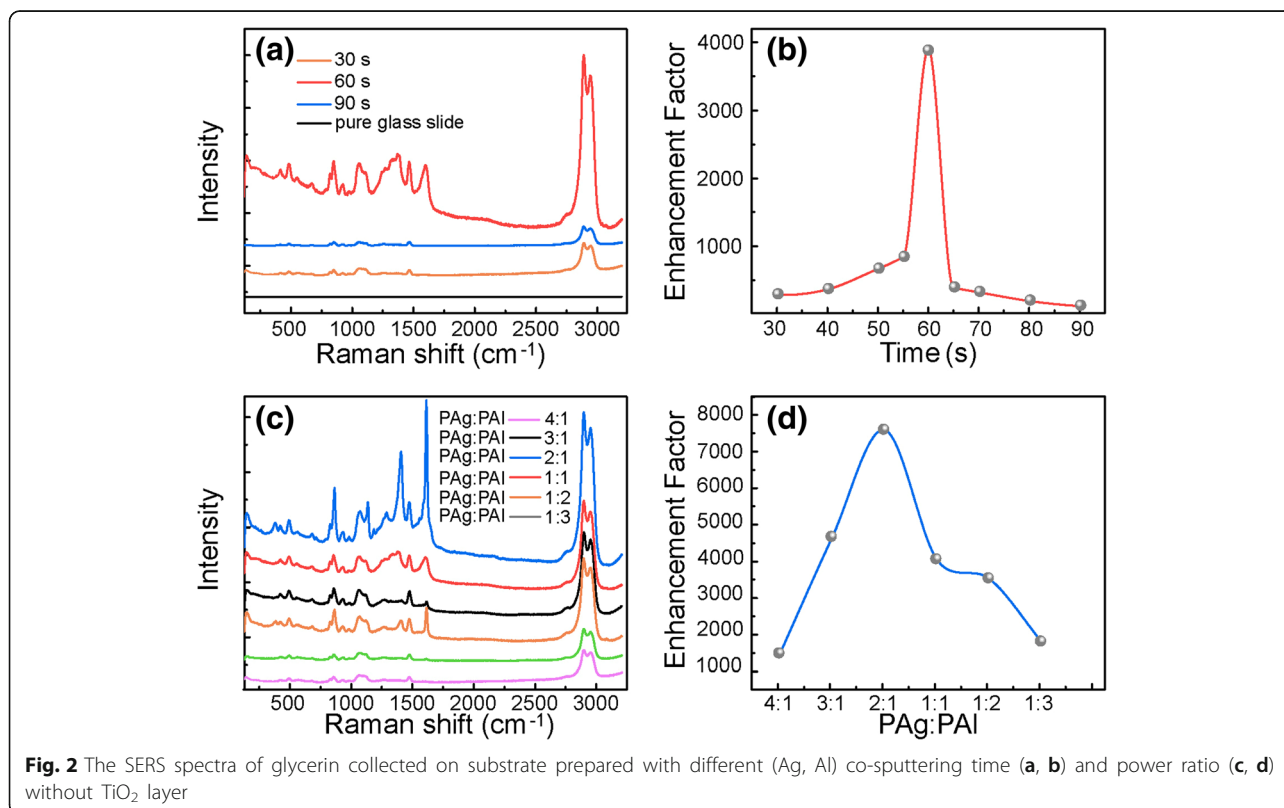
Results and Discussion
In our SERS substrate, Ag NPs act as our SERS active moiety due to its high recorded enhancement factor. To prepare Ag NPs on pre-cleaned glass, aluminum was co-sputtered with silver target together firstly. Then, phosphate was used to remove Al NPs to form uniform Ag NPs on the glass. After this, an ultrathin TiO$_2$ layer was coated to the Ag NP surface without pretreatment via ALD. The schematic illustration of the whole fabrication process is displayed in Fig. 1. All the preparation details have been given in the "Methods" section.
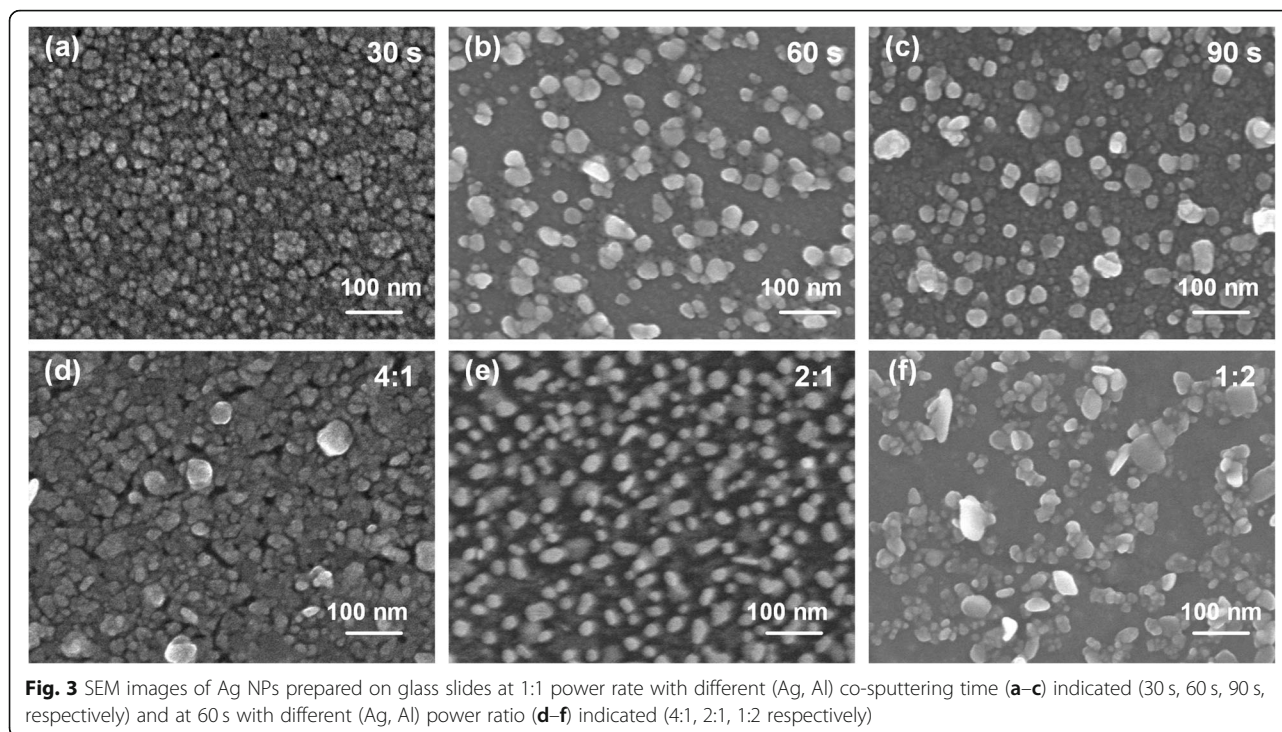
The Raman measurement was carried out by adding an equal amount of glycerol solution (usually 0.1 mL 10% glycerol solution) on all prepared SERS substrates. Noticeably, the co-sputtering time and power ratio of silver and aluminum play important roles in adjusting the size and distribution of uniform Ag NPs on the glass slide, which result in a great difference of SERS performance as well as

Fig. 1 Scheme of highly sensitive SERS substrate fabricated by co-sputtering and atomic layer deposition on glass slides

confirming the active moiety of Ag NPs. For comparison, we investigated the influence of co-sputtering time and power ratio (silver and aluminum) on the signal enhancement factor (EF) of substrates without TiO_2 layer, separately. As is shown in Fig. 2a and b, the glycerol Raman signals become stronger and stronger with the increasing co-sputtering time and reach a peak value at the point of 60 s with a constant 1:1 power ratio of silver and aluminum target (30 W) during the substrate deposition process. As the sputtering time continues to extend, the EF presents a sharp decrease. The deposition rate, determined by stylus profile meter on thick calibration sample, is 0.14 nm/s.

Fig. 2 The SERS spectra of glycerin collected on substrate prepared with different (Ag, Al) co-sputtering time (**a**, **b**) and power ratio (**c**, **d**) without TiO_2 layer

Fig. 3 SEM images of Ag NPs prepared on glass slides at 1:1 power rate with different (Ag, Al) co-sputtering time (**a**–**c**) indicated (30 s, 60 s, 90 s, respectively) and at 60 s with different (Ag, Al) power ratio (**d**–**f**) indicated (4:1, 2:1, 1:2 respectively)
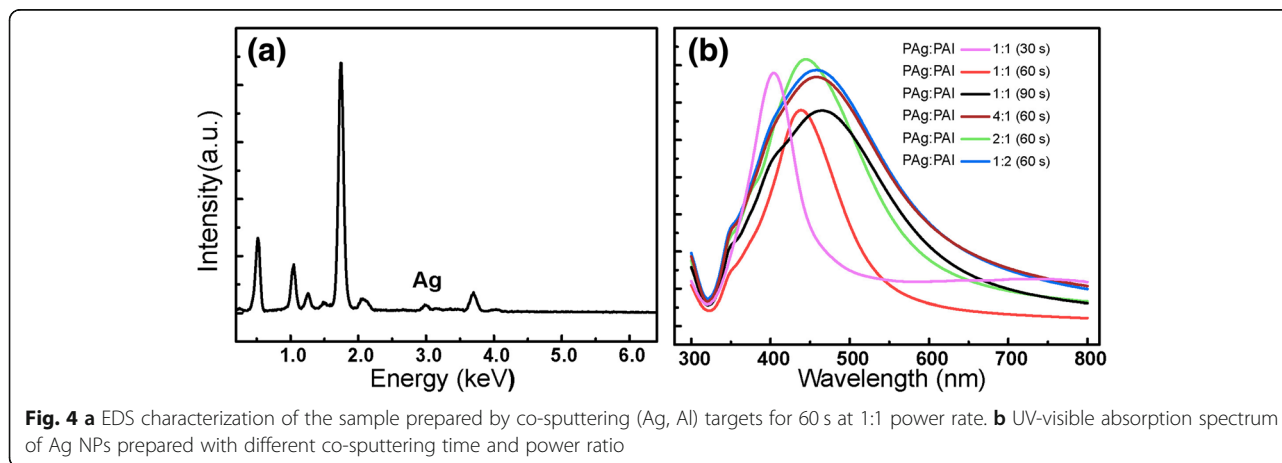
Based on this, we also display the obtained Raman spectrum and EF dependence on aluminum content in Fig. 2c and d. During the co-sputtering process, the aluminum content was modulated by adjusting the sputtering power of aluminum target with a fixed sputtering time (60 s). The Raman signal gets stronger with the increasing aluminum content first and reaches peak value at 2:1 sputtering power ratio of silver and aluminum target. The average film thickness of the sample with the best SERS performance is about 7.2 nm, calculated from the deposition rate determined the same way. Then, the EF will attenuate as the aluminum content continues to increase. The dependence of EF on both co-sputtering time and power ratio (aluminum content) is ascribed to

their efficient modulation on the size and distribution of Ag NPs. As is known, both the size and distribution of Ag NPs contribute a lot to generate hot spots in local electromagnetic (EM) field among Ag NPs, which resulted in the SERS activity [15, 26–28].

In Fig. 3, we present SEM images of Ag NPs prepared with different (Ag, Al) co-sputtering time and power ratio. The substrate with the best performance also shows a more uniform size and distribution of Ag NPs, as displayed in Fig. 3e. This also confirms their influence on SERS performance. In fact, both Ag and Al particles grow larger and faster with the augment of sputtering time and power. This is the reason why we can modulate the size and distribution of Ag NPs by co-sputtering
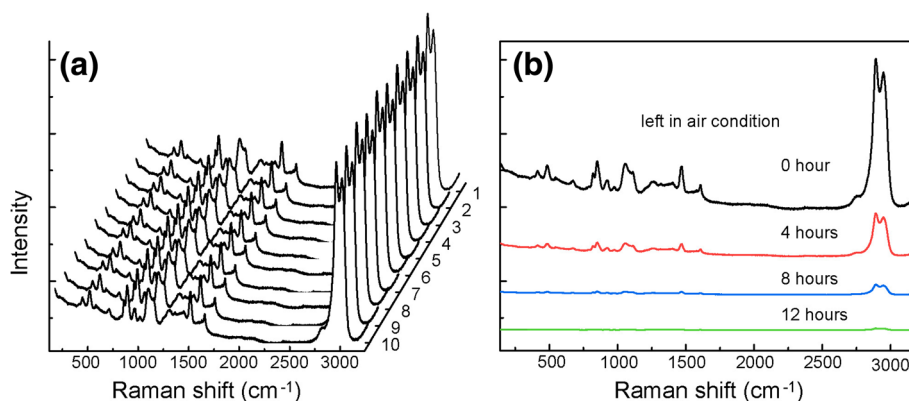

Fig. 4 a EDS characterization of the sample prepared by co-sputtering (Ag, Al) targets for 60 s at 1:1 power rate. **b** UV-visible absorption spectrum of Ag NPs prepared with different co-sputtering time and power ratio

Fig. 5 The SERS spectra of glycerin collected from **a** 10 random points on the substrate as soon as well-prepared. **b** The same position on the substrate after different time left in air condition

with Al and removing it later [15, 26, 27]. It is note-worthy that compared with the samples prepared by sputtering single silver target, this co-sputtering method has significantly improved the SERS performance.

To confirm the Ag NPs as SERS active moiety, EDS characterization of the sample prepared by co-sputtering (Ag, Al) targets for 60 s at 1:1 power rate is exhibited as Fig. 4a. Besides, The UV-Vis absorption spectrum of the samples prepared by modulating co-sputtering time and (Ag, Al) power ratio is displayed in Fig. 4b. The absorption peaks varied from 404 (co-sputtering 30 s with 1:1 power ratio) to 468 nm (co-sputtering 60 s with 4:1 power ratio), which further certified the influence of size and distribution of Ag NPs on the absorption spectrum, indicating the size and distribution of Ag NP modulation during the deposition process [29].

The uniform distribution of Ag NPs-based active moiety leads to high reproducibility of SERS performance. As is exhibited in Fig. 5a, the Raman spectra of the glycerol solution obtained from ten random spots are demonstrated. Each spot displays a distinctive Raman intensity for

glycerin solution each time, confirming the excellent uniformity of the SERS performance. However, the substrate did show a serious problem in further experiments. As Fig. 5b presented, the intensity became weaker and weaker when it was left in air condition. It implied that the substrate gradually lost SERS activity, which was attributed to the easy oxidation of Ag NPs [13].

To improve the stability of the SERS substrate, different thin oxide layers were coated on the Ag NPs via ALD [17, 21, 30, 31]. Different from the mechanism behind Al_2O_3 and SiO_2 layer, which is ascribed to the long-range effect of the enhanced electromagnetic field generated by the encapsulated Ag NPs, TiO_2 was chosen here due to its additional contribution in SERS performance via chemical effect besides the long-range effect [32]. According to the result given in Fig. 6a, it can be clearly seen that the substrate with 2 nm TiO_2 further enhances the Raman signal of glycerin significantly. Besides, the SERS performance is closely related with the thickness of oxide layer. As the thickness of TiO_2 increases, the intensity of the
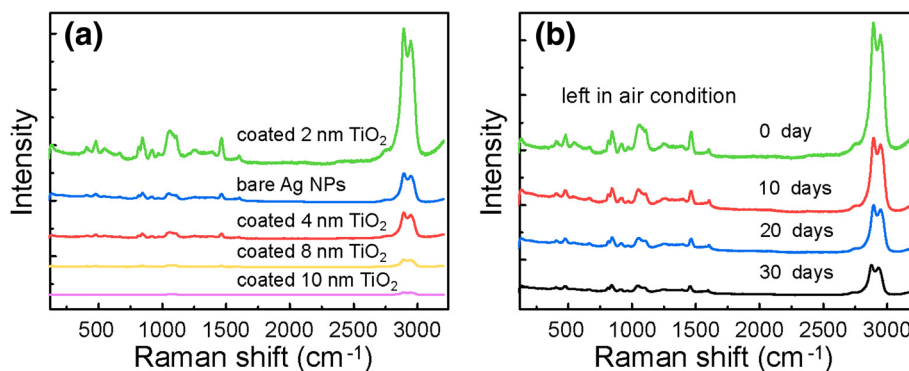

Fig. 6 Comparison of SERS glycerin spectra collected from **a** uncoated Ag NPs on glass sides and coated with TiO_2 of different thickness. **b** The substrate coated a 2-nm TiO_2 film in different duration left in air condition

Yin *et al. Nanoscale Research Letters*   (2019) 14:168

Page 6 of 7

Raman signal attenuates quickly. This is in accordance with previous reports and could be well explained by the exponential attenuation of a strong electromagnetic field with the increasing thickness of the "spacer" film [31]. The stability was evaluated by comparing the SERS performance of the substrate in different duration, which was left in air condition since it was prepared. As is shown in Fig. 6b, the SERS spectra still display distinctive intensity for glycerin solution even 30 days later, which further confirms the ultrathin TiO_2 a protective layer.

Conclusion

In summary, we develop a facile method to fabricate highly sensitive and stable Ag NP-based SERS substrate in glycerol detection by combining co-sputtering and ALD technology, which play an important role in super lubricating solutions. By modulating both sputtering and power ratio during the co-sputtering process, well-distributed Ag NPs on glass slides were obtained as SERS active moiety, which presented highly sensitive SERS performance. The stability of SERS substrate is significantly improved by coating an ultrathin TiO_2 layer via ALD to impede surface oxidation and prohibit aggregation of Ag NPs. Besides, an interesting phenomenon is that the TiO_2 layer could further enhance the Raman signal with proper thickness. We ascribe this to the contribution of chemical effect and the influence of "spacer film" on the electromagnetic field generated by the Ag NPs. This might highlight the application of SERS in interface state investigation to explore novel liquid lubricating materials.

Abbreviations
ALD: Atomic layer deposition; FE-SEM: Field emission scanning electron microscopy; NPs: Nanoparticles; SERS: Surface-enhanced Raman scattering

Availability of Data and Materials
All data generated or analyzed during this study are included in this published article.

Authors' Contributions
GLY and SHB carried out the experiment and drafted the manuscript. XLT, ZL, and YPZ completed the SEM and Raman spectroscopy characterization. JL and DNH designed the experiment. WMW and JL were involved in the co-sputtering and atomic layer deposition. All the authors have read and approved the final manuscript.

Competing Interests
The authors declare that they have no competing interests.

Author details
[1]School of Material Science and Engineering, Shanghai Jiao Tong University, No. 800 Dongchuan Road, Shanghai 200240, People's Republic of China. [2]National Engineering Research Center for Nanotechnology, No. 28 East Jiangchuan Road, Shanghai 200241, People's Republic of China. [3]School of Mechanical Engineering, Shanghai Jiao Tong University, No.800 Dongchuan Road, Shanghai 200240, People's Republic of China.

References
1. Fleischmann M, Hendra PJ, McQuillan AJ (May 1974) Raman spectra of pyridine adsorbed at a silver electrode. Chemical Physics Letters 26(2): 163–166
2. Kneipp K et al (1997) Single molecule detection using surface-enhanced Raman scattering (SERS). Physical Review Letters 78(9):1667–1670
3. Cao YWC, Jin R, Mirkin CA (2002) Nanoparticles with Raman spectroscopic fingerprints for DNA and RNA detection. Science 297(5586):1536–1540
4. Camden JP et al (2008) Probing the structure of single-molecule surface-enhanced Raman scattering hot spots. J Am Chem Soc 130(38): 12616–12617
5. Yang L, Ma L, Chen G, Liu J, Tian Z-Q (2010) Ultrasensitive SERS detection of TNT by imprinting molecular recognition using a new type of stable substrate. Chemistry 16(42):12683–12693
6. Savolainen M et al (2009) Better understanding of dissolution behaviour of amorphous drugs by in situ solid-state analysis using Raman spectroscopy. Eur J Pharm Biopharm 71(1):71–79
7. Anderson MS (2000) Locally enhanced Raman spectroscopy with an atomic force microscope. Applied Physics Letters 76(21):3130–3132
8. Wustholz KL et al (2010) Structure-activity relationships in gold nanoparticle dimers and trimers for surface-enhanced Raman spectroscopy. J Am Chem Soc 132(31):10903–10910
9. Langhammer C, Yuan Z, Zorić I, Kasemo B (Apr. 2006) Plasmonic properties of supported Pt and Pd nanostructures. Nano Letters 6(4):833–838
10. Wang Y, Asefa T (2010) Poly(allylamine)-stabilized colloidal copper nanoparticles: Synthesis, morphology, and their surface-enhanced Raman scattering properties. Langmuir 26(10):7469–7474
11. Tang H, Meng G, Huang Q, Zhang Z, Huang Z, Zhu C (2012) Arrays of cone-shaped ZnO nanorods decorated with Ag nanoparticles as 3D surface-enhanced Raman scattering substrates for rapid detection of trace polychlorinated biphenyls. Advanced Functional Materials 22(1):218–224
12. Futamata M, Maruyama Y, Ishikawa M (2003) Local electric field and scattering cross section of Ag anoparticles under surface plasmon resonance by finite difference time domain method. J Phys Chem B 107(31): 7607–7617
13. Wiley B, Sun Y, Xia Y (2007) Synthesis of silver nanostructures with controlled shapes and properties. Acc Chem Res 40(10):1067–1076
14. Seidel J, Grafström S, Eng L (2005) Stimulated emission of surface plasmons at the interface between a silver film and an optically pumped dye solution. Phys Rev Lett 94(17):177401
15. Santoro G et al (2014) Silver substrates for surface enhanced Raman scattering: correlation between nanostructure and Raman scattering enhancement. Applied Physics Letters 104:243107
16. Gutes A, Carraro C, Maboudian R (2009) Silver nanodesert rose as a substrate for surface-enhanced Raman spectroscopy. ACS Appl Mater Interfaces 1(11):2551–2555
17. Formo EV, Mahurin SM, Dai S (2010) Robust SERS substrates generated by coupling a bottom-up approach and atomic layer deposition. ACS Appl Mater Interfaces 2(7):1987–1991
18. Kang Y et al (2017) In situ preparation of Ag nanoparticles by laser photoreduction as SERS substrate for determination of Hg^{2+}. J Raman Spectroscopy 48(3):399–404
19. McLellan JM, Li ZY, Siekkinen AR, Xia Y (2007) The SERS activity of a supported ag nanocube strongly depends on its orientation relative to laser polarization. Nano Letters 7(4):1013–1017

20. Zhang C et al (2015) SERS detection of low-concentration adenosine by silver nanoparticles on silicon nanoporous pyramid arrays structure. Applied Surface Sci 347:668–672
21. Zhang Z, Yu J, Yang J, Lv X, Wang T (2015) Preparation of sensitive and recyclable porous Ag/TiO$_2$ composite films for SERS detection. Applied Surface Sci 359:853–859
22. Xia N, Cai Y, Jiang T, Yao J (Aug. 2011) Green synthesis of silver nanoparticles by chemical reduction with hyaluronan. Carbohydrate Polymers 86(2):956–961
23. Roth SV et al (2011) In situ observation of cluster formation during nanoparticle solution casting on a colloidal film. J Phys: Condensed Matter 23(25):254208
24. Li J, Zhang C, Luo J (2013) Superlubricity achieved with mixtures of polyhydroxy alcohols and acids. Langmuir 29(17):5239–5245
25. Li J, Zhang C, Luo J (Aug. 2011) Superlubricity behavior with phosphoric acid–water network induced by rubbing. Langmuir 27(15):9413–9417
26. Schwartzkopf M et al (2013) From atoms to layers: in situ gold cluster growth kinetics during sputter deposition. Nanoscale 5(11):5053–5062
27. Schwartzkopf M et al (2017) Role of sputter deposition rate in tailoring nanogranular gold structures on polymer surfaces. ACS Applied Materials & Interfaces 9(6):5629–5637
28. Stamplecoskie KG, Scaiano JC, Tiwari VS, Anis H (2011) Optimal size of silver nanoparticles for surface-enhanced Raman spectroscopy. The Journal of Physical Chemistry C 115(5):1403–1409
29. Schwartzkopf M et al (Jun. 2015) Real-time monitoring of morphology and optical properties during sputter deposition for tailoring metal–polymer interfaces. ACS Applied Materials & Interfaces 7(24):13547–13556
30. Hu X et al (2012) Large-scale homogeneously distributed Ag-NPs with sub-10 nm gaps assembled on a two-layered honeycomb-like TiO$_2$ film as sensitive and reproducible SERS substrates. Nanotechnology 23(38):385705
31. Li JF et al (2010) Shell-isolated nanoparticle-enhanced Raman spectroscopy. Nature 464(7287. Nature Publishing Group):392–395
32. Musumeci A et al (2009) SERS of semiconducting nanoparticles (TiO$_2$ hybrid composites). J Am Chem Soc 131(17):6040–6041